

Neural Image Inpainting Guided with Descriptive Text

Lisai Zhang, Qingcai Chen*, Baotian Hu and Shuoran Jiang

Harbin Institute of Technology, Shenzhen

lisaizhang@foxmail.com, qingcai.chen@hit.edu.cn, {baotianchina, shaunbysn}@gmail.com

Abstract

Neural image inpainting has achieved promising performance in generating semantically plausible content. Most of the recent works mainly focus on inpainting images depending on vision information, while neglecting the semantic information implied in human languages. To acquire more semantically accurate inpainting images, this paper proposes a novel inpainting model named *Neural Image Inpainting Guided with Descriptive Text* (NIGDT). First, a dual multi-modal attention mechanism is designed to extract the explicit semantic information about corrupted regions. The mechanism is trained to combine the descriptive text and two complementary images through reciprocal attention maps. Second, an image-text matching loss is designed to enforce the model output following the descriptive text. Its goal is to maximize the semantic similarity of the generated image and the text. Finally, experiments are conducted on two open datasets with captions. Experimental results show that the proposed NIGDT model outperforms all compared models on both quantitative and qualitative comparison. The results also demonstrate that the proposed model can generate images consistent with the guidance text, which provides a flexible way for user-guided inpainting. Our systems and code will be released soon.

1 Introduction

Image inpainting plays an important role in many tasks, such as restoration of damaged paintings, photo editing and image rendering [Bertalmio *et al.*, 2000]. It requires generating visually realistic content in missing regions while keeping coherence [Ma *et al.*, 2019]. Recently, there have been many methods proposed for generating semantically plausible and diverse contents, such as integrating context [Liu *et al.*, 2019] and estimating the distribution of missed regions [Zheng *et al.*, 2019].

Most image inpainting works are focused on the input image itself, which is based on the assumption that the miss-



Figure 1: Demo of image inpainting for unique area, where (a) is NIGDT with truth text and (b) is NIGDT image editing with altered text. (Better view with zoom in.)

ing area should have similar patterns with the background region. Based on this assumption, diffusion-based [Bertalmio *et al.*, 2002] and patch-based [J. Weickert, 1999] models are proposed to use the remaining image to recover the missed regions. These models produce high quality images, but usually make critical failures in complicated scenes such as mask on objects or large holes [Yeh *et al.*, 2017]. In recent years, deep learning based image inpainting methods have been presented to overcome this limitation [Yeh *et al.*, 2017]. [Pathak *et al.*, 2016] firstly proposed an encoder-decoder structure with Generative Adversarial Networks (GAN). To improve the ability of encoding the input image, [Iizuka *et al.*, 2017] adopted dilated convolutions and proposed global and local discriminators and generate photorealistic results. However, the model has limitations of filling irregular holes. The latest works on neural image inpainting have achieved credible generation quality on irregular masks from the perspective of improving convolution [Yu *et al.*, 2019; Ma *et al.*, 2019] and integrating context features [Liu *et al.*, 2019]. Generating a diverse set of inpainting results is also an important research direction. The latest model is the PICNet [Zheng *et al.*, 2019], which proposed a dual pipeline training architecture to learn distribution for the masked area. The model can generate diverse plausible content for a single masked input.

Giving external guidance to inpainting models is a commonly used solution for controlling generation. Some user-guided image inpainting approaches allow external guidance, such as line [Yu *et al.*, 2019] and edges [Nazeri *et al.*, 2019] and exemplar [Vivek Kwatra and Kwatra, 2005] but these guidances are limited to specific graphics tips and lacks semantic diversity.

Since image semantics can be described as descriptive text in most cases, it would be plausible if inpainting models bor-

*Contact Author

row necessary semantic information from text descriptions. For example, in Fig. 1, when a text description is given, the target of the model becomes clear and the model output becomes controllable. However, to the best of our knowledge, there is still no work incorporating text into the image inpainting model to guide the generation.

In this paper, we focus on incorporating descriptive text into the neural image inpainting model. The main contributions of this paper are given below:

1) We propose a novel neural image inpainting model that fills the holes of an image with the guidance of descriptive text.

2) We propose a novel dual multi-modal attention mechanism to exploits the semantically features about the masked region from the descriptive text.

3) We design an image-text matching loss to regularize the similarity of text and model output and enforce the generated image following the descriptive text.

Experimental results of quantitative and qualitative comparison show that the proposed NIGDT model outperforms state-of-the-art models on open datasets with captions, and the generated results are semantically consistent with the guidance text.

2 Related Work

Our research builds on previous works in the field of image inpainting and text to image synthesis.

Traditional diffusion-based or patch-based approaches [Bertalmio *et al.*, 2002; J.Weickert, 1999] fill in missing regions by propagating neighboring information or copying from similar patches of the background based on low-level features. These methods work well for surface textures synthesis but often fail on non-stationary textural images. To address the problem, Simakov *et al.* propose a bidirectional similarity synthesis approach [Yuhang Song and Jay, 2018] to better capture non-stationary information, but lead to high algorithm complexity. Recently, deep learning models are introduced to image inpainting that directly generates pixel values of the hole. Context encoders [Pathak *et al.*, 2016] firstly use the encoder-decoder structure and conditional generative adversarial network to image inpainting task. Further, contextual attention [Yu *et al.*, 2018] is proposed for capturing long-range spatial dependencies. To improve the performance on irregular masks, partial convolution [Liu *et al.*, 2018] is proposed where the mask is updated and convolution weights are re-normalized with layers. However, it has limitations to capture detailed information of the masked area in deep layers. For this, [Yu *et al.*, 2019] presents to use gated convolution for free-form image inpainting where a gate network learns the shape of mask in convolution. These approaches can produce only one result for each incomplete image. Thus [Zheng *et al.*, 2019] introduces a CVAE based pluralistic image completion approach. During inference, the model firstly obtains the distribution for the input, then sample various representation vectors from the distribution, and feed these vectors to the decoder to get a variety of outputs.

Many user-guided inpainting methods are explored to enhance image inpainting systems, including dots or lines,

structures, transformation or distortion, and exemplars concluded in [Yu *et al.*, 2019]. Recent advances in conditional generative networks empower user-guided inpainting and synthesis. Wang *et al.* [Ting-Chun Wang and Catanzaro, 2018] propose to synthesize high-resolution photo-realistic images from semantic label maps using conditional generative adversarial networks. [Yu *et al.*, 2019] extend their model to support user-guided inpainting with sketches. Another related work [Li *et al.*, 2019b] explored an image manipulation approach through text guidance. However, image inpainting guided with text is still challenging in two aspects: Firstly, image and text are heterogeneous, it is hard to transform image and text features to share space. What's more, the descriptive text usually contains redundant information, the model must distinguish the information about the corrupted region from the text.

Text to image synthesis directly generates an image from the text description. Here we selectively review several related work. [S. Reed and Lee, 2016a] first showed that the conditional GAN was capable of synthesizing plausible images from text descriptions. [S. Reed and Lee, 2016b] stacked several GANs for text-to-image synthesis. However, their methods are conditioned on the global sentence vector, missing fine-grained word-level information. AttnGAN [Xu *et al.*, 2018] develops word and sentence level matching network to generate fine-grained images from text. [Li *et al.*, 2019a] proposed to exploit word-level information during synthesis through attention mechanism.

3 Approach

Our proposed NIGDT can be formulated as follows: given the masked input image \mathbf{I}_m and descriptive text \mathbf{T} the model output the target image \mathbf{I}_g . The overall structure of our model is shown in Figure 2. It composes of three parts: Encoders for Image and Text, Dual multi-modal Attention and Inpainting Generation.

3.1 Encoders for Image and Text

The input image extract image representations with a 7-layer resnet. To obtain the image representations of low-level and high-level, we take the outputs of the last two layers as Eq. 2

$$v_l, v_h = \text{Enc}_{img}(\mathbf{I}_m) \quad (1)$$

where Enc_{img} denotes the image encoder, v_h is the high-level representation output by the last layer, v_l is the output of the second last layer. v_l will be fed directly to the generator to reconstruct the unmasked areas.

As for the input sentence, we use a text encoder to compute a sequence of word representations and a sentence representation as Eq. 2

$$t_{sent}, t_{wrd} = \text{Enc}_{txt}(\mathbf{T}) \quad (2)$$

where Enc_{txt} denotes the image encode, t_{wrd} is word representation vectors, t_{sent} is sentence representation vectors. Enc_t is a GRU network with 256 hidden size.

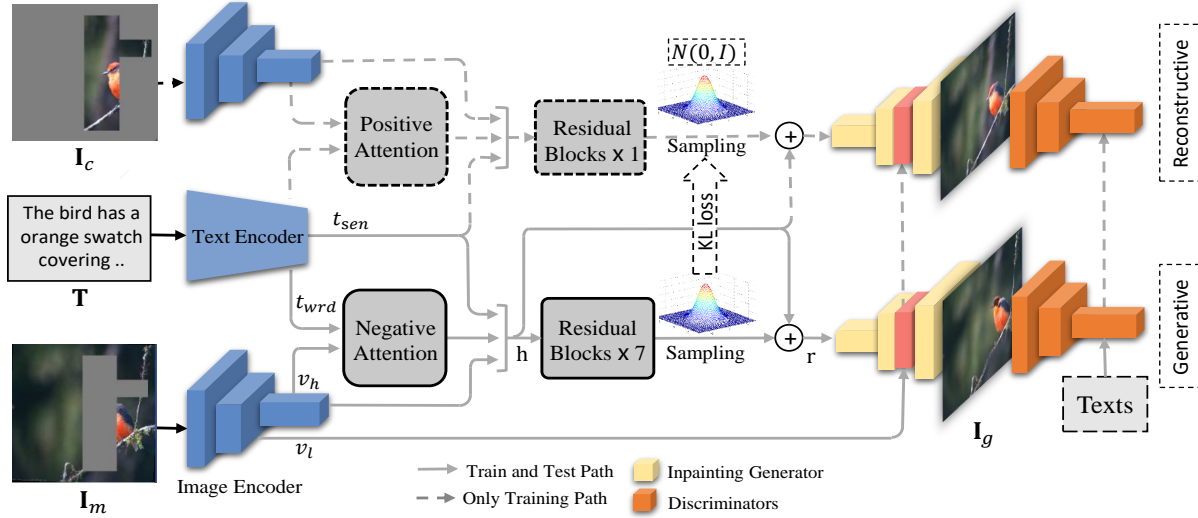


Figure 2: Overall structure of NIGDT model.

3.2 Dual Multi-modal Attention Mechanism

Extending traditional attention schema [Bahdanau *et al.*, 2014], we propose a dual multi-modal attention mechanism to capture the relation between query and complementary contents shown in Fig. 3. In the NIGDT model, the goal of dual multi-modal attention mechanism is to extract the semantic information about the masked area from the text. Our *key insight* is: assuming the input image I_m and its counterpart I_c are complementary, then we can obtain the information about I_c by dismissing the overlap information between T and I_m . Therefore, we construct a dual pair with I_m and I_c , where I_c is available only during training. It is called dual pair because we calculate the attention weights on these two inputs reciprocally. To formulate, we use x^p to denote the variable x only appears in the positive attention path, and x^n for the negative attention path.

We extract the high-level visual representation v_h^p of I_c through Enc_{img} , and then transform the visual representation with 1×1 convolution. As the dotted line path in Fig 3, we then compute the attention weights between v_h^p and word representations t_{wrd} . When computing the attention weights we keep the mask from the input and apply it to the feature map on the same region. The computing is formulated as Eq. 3:

$$\hat{s}_{i,j} = M_i^p Q(v_{hi}^p)^T t_{wrdj} \quad (3)$$

where $Q(v_h) = Wv_h$, and W is an 1×1 convolution filter, M^p is the binary mask (the value for masked pixels is 0 and elsewhere is 1).

As the bold line path in Fig 3, we then calculate attention weights between v_h^n and t_{wrd} reciprocally as Eq. 4.

$$s_{i,j} = -Q(v_{hi}^n)^T t_{wrdj} + M_i^n \quad (4)$$

where M^n is the mask on v_h^n . Specially, in M^n the value for masked pixels is $-\infty$ and elsewhere is 0.

Attention weights on both paths are fed to softmax as Eq. 5

$$\beta_{j,i} = \frac{\exp(s_{i,j})}{\sum_{i=1}^N \exp(s_{i,j})} \quad (5)$$

where N is the area of the feature map, β denotes the reciprocal attention map. The word representations are then weighted by multiplying the attention map as Eq. 6:

$$t_{ei} = \sum_{j=1}^L \beta_{i,j} t_{wrdj} \quad (6)$$

where L is the length of sentence, t_e are the weighted word representations.

There is still a problem for the negative attention path: vectors in t_e are distributed following the content in v_h , so the values of the masked region in t_e are zero, making it hard to be decoded. To handle this problem, we apply a global maxpooling to \hat{t}_e . Because the specific location of missing semantic is unknown, we then uniformly replicate the maxpooling output. The calculation is formulated as Eq. 7

$$t_{ej} = \max_{1 \leq i \leq N} \hat{t}_{ei} \quad (7)$$

where N is the area of feature map, t_e is the extracted word representation.

After extracting word representation through the multi-modal attention, The sentence feature, image feature and extracted word representation are concatenated and fed to a distribution projection network Enc_{proj} to generate a Gaussian distribution, formulated as Eq. 8 and Eq. 9

$$h = [v_h, t_e, t_{sent}] \quad (8)$$

$$\mu, \sigma = \text{Enc}_{proj}(h) \quad (9)$$

where μ and σ are mean and variance of the predicted Gaussian distribution, and h is the multi-modal hidden representations, Enc_{proj} denotes distribution projection, which consists of 5-layer residual blocks. Finally, we combine the multi-modal hidden representations and sampled representation with a residual connection as in Eq. 10,

$$r = h + \text{Gaussian}(\mu, \sigma) \quad (10)$$

where r is the multi-modal representation.

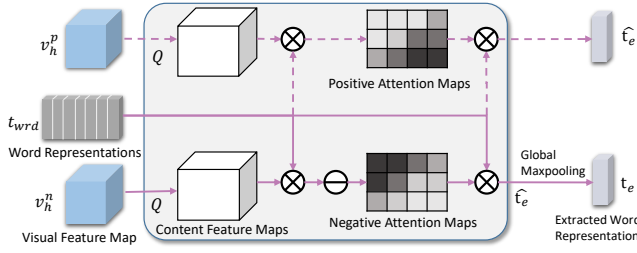


Figure 3: Diagram of the Dual Multi-modal Attention.

3.3 Inpainting Generation

The output image is generated based on multi-modal representation r through a 5-layer residual network with spectral normalization [Miyato T, 2018]. We feed the low-level image feature v_l to the generator through a high way path based on short long term attention as [Zheng *et al.*, 2019]. The short long term attention firstly computes a weight map through self-attention on the decoder feature map, and then obtain short and long term attention features by multiply attention feature map on decoder and encoder feature maps. The generator then combines these two attention features to residual generation layers and output a complete image I_g .

To enforce the model generating image following the semantic guidance of text, we pre-train two match networks that measures text-image similarity in text and sentence level. Using the match network like a discriminator, we construct match loss to refines semantic relation of text and image output by maximizing similarity score, which is formulated as Eq. 11.

$$\mathcal{L}_T = D_3(t_{wrd}, I_g) + D_4(t_{sent}, I_g) \quad (11)$$

where \mathcal{L}_T denotes match loss, D_3 and D_4 denote the word and sentence level match network. The pre-train follows the same procedure in AttnGAN [Xu *et al.*, 2018], but remove the image-label match term and only use match text and image output, because labels are in-available in inpainting task.

For image appearance quality, we use reconstruction and adversarial losses. Three loss functions are applied as Eq. 12:

$$\mathcal{L}_I = \|I - I_g\|_1 + \|D_1(I) - D_1(I_g)\|_2 + [D_2(I_g) - 1]^2 \quad (12)$$

where D_1 is a discriminator that return feature of the final layer. D_2 is based on the loss in LSGAN [Xudong Mao and Smolley, 2017] which encourage the generator create real world like image.

3.4 Objective

Our model is trained with a dual pipeline shown as Fig. 2. During training, the model not only restores the complete image from the corrupted image I_m , but also from its counterpart I_c . This auxiliary path is named reconstructive path because information of the full images is available. In principle, the reconstructive path could learn the complete distribution of the full image, and guide the generative path optimization. To formulate, in this subsection we use ' x^r ' to denote "variable x in the reconstructive path" and ' x^g ' to denote "variable x in the generative path".

The data flow of reconstructive path is almost the same as generative path, except for the dual multimodal attention (as in Eq.3) and multi-modal representation. The multi-modal hidden feature in residual connection of reconstructive path comes from h^g , formulated as Eq. 13:

$$r^r = h^g + \text{Gaussian}(\mu^r, \sigma^r) \quad (13)$$

Based on the dual pipeline, the NIGDT model learn the distribution of image base on a CVAE [Doersch, 2016] probabilistic framework. The conditional variational lower bound of reconstructive path is formulated as Eq. 14:

$$\log p(I_c | h^r) \geq -\text{KL}(q_\psi(\mathbf{z} | I_c, h^r) || p_\phi(\mathbf{z} | h^r)) + \mathbb{E}_{q_\psi(\mathbf{z} | I_c, h^r)} [\log p_\theta(I_c | \mathbf{z})] \quad (14)$$

where \mathbf{z} is the latent vector, $q_\psi(\cdot | \cdot)$ denotes posterior sampling function, $p_\phi(\cdot | \cdot)$ denotes the conditional prior, $p_\theta(\cdot | \cdot)$ denotes the likelihood, with ψ , ϕ and θ being the deep network parameters of their corresponding functions.

Similarly, for generative path we have the lower bound as Eq. 15:

$$\log p(I_c | h^g) \geq -\text{KL}(q_\psi(\mathbf{z} | I_c, h^g) || p_\phi(\mathbf{z} | h^g)) + \mathbb{E}_{q_\psi(\mathbf{z} | I_c, h^g)} [\log p_\theta(I_c | \mathbf{z})] \quad (15)$$

However, $q_\psi(\mathbf{z} | I_c, h^g)$ can not be calculated directly because I_c is not available in generative path. We assume that h^r is approximate to h^g after optimizing encoders, and have $q_\psi(\mathbf{z} | I_c, h^r) \approx q_\psi(\mathbf{z} | I_c, h^g)$, so Eq. 15 is updated as Eq. 16:

$$\log p(I_c | h^g) \geq -\text{KL}(q_\psi(\mathbf{z} | I_c, h^r) || p_\phi(\mathbf{z} | h^g)) + \mathbb{E}_{q_\psi(\mathbf{z} | I_c, h^g)} [\log p_\theta(I_c | \mathbf{z})] \quad (16)$$

The parameters of the NIGDT model are learnt by maximizing these two lower bound. Assuming prior distributions of $p_\theta(\mathbf{z} | h^r)$ and $p_\theta(\mathbf{z} | h^g)$ are Gaussian, for the reconstructive path, the distribution loss is formulated as Eq. 17:

$$\mathcal{L}_{KL}^r = -KL(q_\psi(\mathbf{z} | I_c, h^r) || \mathcal{N}(0, 1)) \quad (17)$$

As for the generative path, \mathcal{L}_{KL} steer prior to close reconstructive path posterior, which can be formulated as Eq. 18:

$$\mathcal{L}_{KL}^g = -KL(q_\psi(\mathbf{z} | I_c, h^r) || p_\theta(\mathbf{z} | h^g)) \quad (18)$$

Overall, the total loss function could be formulated as Eq. 19:

$$\mathcal{L} = \lambda_{KL}(\mathcal{L}_{KL}^r + \mathcal{L}_{KL}^g) + \lambda_I \mathcal{L}_I + \lambda_T \mathcal{L}_T \quad (19)$$

where \mathcal{L}_{KL} regularizes KL divergence of prior and posterior distribution, \mathcal{L}_I maximize the expectation term from image quality and \mathcal{L}_T regularise text-image semantic similarity.

4 Experiments

4.1 Datasets

We evaluate our method on image captioning datasets CUB [Wah *et al.*, 2011] and COCO [Lin *et al.*, 2014], and use their original train, test and validation split. There are ten sentences per image in CUB and five in COCO. To further explore the inpainting quality of unique regions, we introduce *object mask* based on object boxes label on CUB. Completion of object mask regions is more challenging because of their uniqueness.

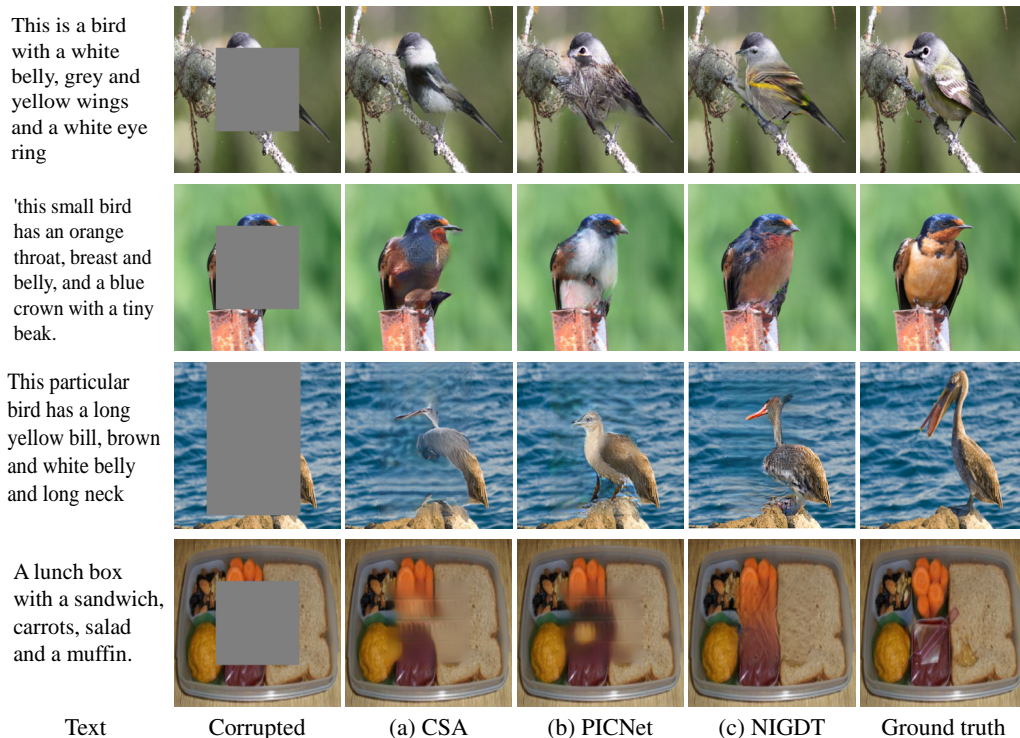


Figure 4: Qualitative comparisons on CUB and COCO validation sets. Best viewed with zoom-in.

4.2 Implement Details

For images in both CUB and COCO datasets, we resize each training image to make its minimal length/width as 256 and crop the sub-image of size 256x256 at the center. All networks were initialized with orthogonal initialization [Saxe *et al.*, 2013] and trained end-to-end with a learning rate of 10^{-4} and Adam optimizer [Kingma and Ba, 2014]. Match networks are pre-trained as in [Xu *et al.*, 2018] on CUB and COCO respectively. During training, the weights of loss function terms are set as $\lambda_{KL} = \lambda_I = 20$, $\lambda_T = 0.5$. Experiments are conducted on Ubuntu 18.04 system, with i7-9700K 3.70GHz CPU and 11G NVIDIA 2080Ti GPU.

We compare the proposed NIGDT model with two state-of-the-art methods PICNet [Zheng *et al.*, 2019] and CSA [Liu *et al.*, 2019] base on their official source code¹.

4.3 Quantitative Results

It has been mentioned [Yu *et al.*, 2018; Yu *et al.*, 2019] that image inpainting lacks good quantitative evaluation metrics. Still, we select commonly used mean ℓ_1 loss, peak signal-to-noise ratio (PSNR), total variation (TV) and Structural Similarity (SSIM) for quantitative comparison. We will further discuss the semantic consistency of results in qualitative.

As the results in Table 1, the proposed NIGDT model outperforms state-of-the-art models on object mask in all measures, proving that this text-guided model works well in filling holes on such unique areas. On CUB and COCO dataset

Mask	Model	$\ell_1 \downarrow$	PSNR \uparrow	TV loss \downarrow	SSIM \uparrow
Object (CUB)	CSA	15.85	19.13	8.33	0.689
	PIC	17.12	18.31	8.35	0.660
	NIGDT	14.70	19.45	8.26	0.700
Center (CUB)	CSA	7.99	20.95	9.51	0.824
	PIC	8.58	20.51	9.79	0.822
	NIGDT	8.34	20.98	9.44	0.823
Center (COCO)	CSA	7.73	21.57	9.79	0.824
	PIC	7.78	21.51	9.87	0.836
	NIGDT	7.99	21.18	9.51	0.842

Table 1: Quantitative comparison with state-of-the-art on CUB and COCO dataset. \downarrow means lower is better, \uparrow means higher is better.

with the center mask, our model achieves comparable performance than these two inpainting models but does not exceed these models on two pixel-wise independence measures, which also explain our assumption because not all regions under the center mask are unique to surroundings and mentioned in the text. It is worth noting that the performance of all evaluated models decreases on object masked samples, while our model has the least performance degradation.

4.4 Qualitative Results

Fig. 4 shows the qualitative results on the CUB and COCO validation set. As shown in the figure, the results of all the three models on the CUB dataset are photographic, but the CSA and PICNet fail to recover special characteristics in the original image, such as the belly color and neck shape.

¹ <https://github.com/KumapowerLIU/CSA-inpainting>
<https://github.com/lyndonzheng/Pluralistic-Inpainting>

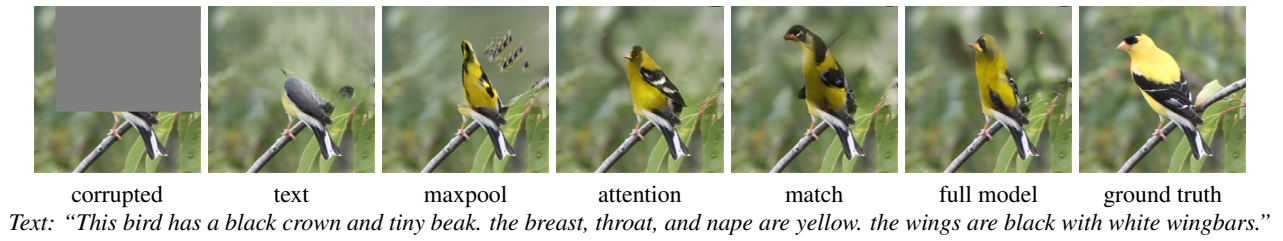


Figure 5: The effect of different components in our model on CUB dataset.



"The bird has a **black** and **white** spotted breast a red hat and grey wings."



"A bird with a white breast and a **brown** crown."



"A distinct red bird with a blue head **blue** wings and a red eyering."
"A distinct red bird with a blue head and **red** wings."

Figure 6: Examples of text-guided image editing.

Through careful observation, it can be found that the content filled by CSA and PICNet has similar characteristics to the surroundings such as color and texture. In comparison, the image generated by the NIGDT model recover these unique features as mentioned in the text and is semantically consistent with the original image. On the challenging COCO dataset, all these three models are imperfect, but our model obtains a better appearance quality.

4.5 User Study

To evaluate the models from human perspective, we conduct a user study through a ranking game. We collect 100 test images with captions with object masks from the CUB validation dataset. For each image, four solutions from (1) Ground truth, (2) Our model, (3) PICNet, (4) CSA model are prepared. We randomly shuffle the four samples and recruit 20 volunteers to rank these four images according to naturalness and the semantic consistency to the text description. On the four solutions, we compute the average of the ranking score. The results are shown in Table 2. According to the results, our model performs better than other models in terms of realistic, and significantly higher in semantic consistency.

Model	Naturalness	Semantic Consistency
Ground Truth	1.208	1.363
CSA	2.981	3.060
PICNet	3.178	3.469
NIGDT	2.531	2.106

Table 2: Numerical result of user study.

4.6 Discussion

To further explore the usage of our work, we propose an interactive image editing case where users mask the region to be changed and give a text to describe a desired content. As in Figure 6, the top two examples are color variation edit by masking the belly or crown and give a text different from original image semantic. In the third case, we intentionally select a region between two differently colored areas and command the model to fill the hole as neighbor colors separately by two different sentences. The result shows the output qualify the text description and did not be affected by the color of adjacent areas. The experimental results presents a new possible formulation of image editing.

To investigate the effectiveness of our designed components including dual multi-modal attention, maxpooling on weighted word features, cross-modal match loss and text guidance, we trained four models without each component using the same super parameters and epochs. As shown in fig. 5, the model without guidance text provides an incomplete and semantically different solution. Without the maxpooling layer in dual multi-modal attention, the center of the generation area collapsed. When we remove match loss or dual multi-modal attention the models output still obtain the content of text but failed to allocate these characters to the exact location.

5 Conclusion

We proposed a neural image inpainting model guided with descriptive text (NIGDT). A dual multi-modal attention mechanism is integrated to the proposed model to exploit semantic features about the masked region from the descriptive text. What's more, we presented an image-text matching based loss to improve the semantic consistency between inpainting output and the text. The experimental results on public datasets demonstrated that the proposed NIGDT model outperformed compared models, and generated significantly higher semantically consistent inpainting results. For future work, we will focus on inpainting more complex images with the guidance of texts.

References

- [Bahdanau *et al.*, 2014] Dzmitry Bahdanau, Kyunghyun Cho, and Yoshua Bengio. Neural machine translation by jointly learning to align and translate. *CoRR*, abs/1409.0473, 2014.
- [Bertalmio *et al.*, 2000] Marcelo Bertalmio, Guillermo Sapiro, Vincent Caselles, and Coloma Ballester. Image inpainting. In *Proceedings of the 27th annual conference on Computer graphics and interactive techniques*, pages 417–424, 2000.
- [Bertalmio *et al.*, 2002] Marcelo Bertalmio, Luminata Vese, Sapiro T Guillermo, and Stanley Osher. Simultaneous structure and texture image inpainting. *ITIP*, 12(8), 2002.
- [Doersch, 2016] Carl Doersch. Tutorial on variational autoencoders. *arXiv preprint arXiv:1606.05908*, 2016.
- [Iizuka *et al.*, 2017] Satoshi Iizuka, Edgar Simo-Serra, and Hiroshi Ishikawa. Globally and locally consistent image completion. *TOG*, 36:1–14, 07 2017.
- [J.Weickert, 1999] J.Weickert. Coherence-enhancing diffusion filtering. volume 31, page 111–127, 1999.
- [Kingma and Ba, 2014] Diederik P Kingma and Jimmy Ba. Adam: A method for stochastic optimization. *arXiv:1412.6980*, 2014.
- [Li *et al.*, 2019a] Bowen Li, Xiaojuan Qi, Thomas Lukasiewicz, and Philip Torr. Controllable text-to-image generation. In *Advances in Neural Information Processing Systems*, pages 2063–2073, 2019.
- [Li *et al.*, 2019b] Bowen Li, Xiaojuan Qi, Thomas Lukasiewicz, and Philip HS Torr. Manigan: Text-guided image manipulation. *arXiv preprint arXiv:1912.06203*, 2019.
- [Lin *et al.*, 2014] Tsung-Yi Lin, Michael Maire, Serge Belongie, James Hays, Pietro Perona, Deva Ramanan, Piotr Dollár, and C Lawrence Zitnick. Microsoft coco: Common objects in context. In *ECCV*, pages 740–755. Springer, 2014.
- [Liu *et al.*, 2018] Guilin Liu, Fitsum Reda, Kevin Shih, Ting-Chun Wang, Andrew Tao, and Bryan Catanzaro. Image inpainting for irregular holes using partial convolutions. In *ECCV*, page 85–100, 2018.
- [Liu *et al.*, 2019] Hongyu Liu, Bin Jiang, Yi Xiao, and Chao Yang. Coherent semantic attention for image inpainting. In *ICCV*, October 2019.
- [Ma *et al.*, 2019] Yuqing Ma, Xianglong Liu, Shihao Bai, Lei Wang, Dailan He, and Aishan Liu. Coarse-to-fine image inpainting via region-wise convolutions and non-local correlation. In *IJCAI*, pages 3123–3129, 2019.
- [Miyato T, 2018] Koyama M et al Miyato T, Kataoka T. Spectral normalization for generative adversarial networks. 2018.
- [Nazeri *et al.*, 2019] Kamyar Nazeri, Eric Ng, Tony Joseph, Faisal Qureshi, and Mehran Ebrahimi. Edgeconnect: Generative image inpainting with adversarial edge learning. 2019.
- [Pathak *et al.*, 2016] Deepak Pathak, Philipp Krahenbuhl, Jeff Donahue, Trevor Darrell, and Alexei Efros. Context encoders: Feature learning by inpainting. pages 2536–2544, 06 2016.
- [S. Reed and Lee, 2016a] X. Yan L. Logeswaran B. Schiele S. Reed, Z. Akata and H. Lee. Generative adversarial text-to-image synthesis. 2016.
- [S. Reed and Lee, 2016b] X. Yan L. Logeswaran B. Schiele S. Reed, Z. Akata and H. Lee. Generative adversarial text-to-image synthesis. 2016.
- [Saxe *et al.*, 2013] Andrew M Saxe, James L McClelland, and Surya Ganguli. Exact solutions to the nonlinear dynamics of learning in deep linear neural networks. *arXiv:1312.6120*, 2013.
- [Ting-Chun Wang and Catanzaro, 2018] Jun-Yan Zhu Andrew Tao Jan Kautz Ting-Chun Wang, Ming-Yu Liu and Bryan Catanzaro. High-resolution image synthesis and semantic manipulation with conditional gans. page 8798–8807, 2018.
- [Vivek Kwatra and Kwatra, 2005] Aaron Bobick Vivek Kwatra, Irfan Essa and Nipun Kwatra. Texture optimization for example-based synthesis. volume 24, page 795–802, 2005.
- [Wah *et al.*, 2011] Catherine Wah, Steve Branson, Peter Welinder, Pietro Perona, and Serge Belongie. The caltech-ucsd birds-200-2011 dataset. 2011.
- [Xu *et al.*, 2018] Tao Xu, Pengchuan Zhang, Qiuyuan Huang, Han Zhang, Zhe Gan, Xiaolei Huang, and Xiaodong He. AttnGAN: Fine-grained text to image generation with attentional generative adversarial networks. pages 1316–1324, 06 2018.
- [Xudong Mao and Smolley, 2017] Haoran Xie Raymond YK Lau Zhen Wang Xudong Mao, Qing Li and Stephen Paul Smolley. Least squares generative adversarial networks. In *CVPR*, page 2813–2821, 2017.
- [Yeh *et al.*, 2017] Raymond Yeh, Chen Chen, Teck Lim, Alexander Schwing, Mark Hasegawa-Johnson, and Minh Do. Semantic image inpainting with deep generative models. pages 6882–6890, 07 2017.
- [Yu *et al.*, 2018] Jiahui Yu, Zhe Lin, Jimei Yang, Xiaohui Shen, Xin Lu, and Thomas S Huang. Generative image inpainting with contextual attention. In *CVPR*, pages 5505–5514, 2018.
- [Yu *et al.*, 2019] Jiahui Yu, Zhe Lin, Jimei Yang, Xiaohui Shen, Xin Lu, and Thomas S Huang. Free-form image inpainting with gated convolution. In *CVPR*, pages 4471–4480, 2019.
- [Yuhang Song and Jay, 2018] Zhe Lin Xiaofeng Liu Qin Huang Hao Li Yuhang Song, Chao Yang and CC Jay. Contextual-based image inpainting: Infer, match, and translate. In *ECCV*, page 3–19, 2018.
- [Zheng *et al.*, 2019] Chuanxia Zheng, Tat-Jen Cham, and Jianfei Cai. Pluralistic image completion. In *CVPR*, pages 1438–1447, 2019.